



The 3-Loop Heavy Flavor Corrections to Unpolarized and Polarized Deep-Inelastic Scattering

pdf4lhc meeting, CERN, Genva, December 3, 2024

Johannes Blümlein | November 21, 2024

DESY AND TU DORTMUND

Recent papers:

- J. Ablinger et al., The unpolarized and polarized single-mass three-loop heavy flavor operator matrix elements $A_{gg,Q}$ and $\Delta A_{gg,Q}$, JHEP **12** (2022) 134.
- J. Ablinger et al., The first-order factorizable contributions to the three-loop massive operator matrix elements $A_{Qg}^{(3)}$ and $\Delta A_{Qg}^{(3)}$, Nucl. Phys.B 999 (2024) 116427.
- J. Ablinger et al., The non-first-order-factorizable contributions to the three-loop single-mass operator matrix elements $A_{Qg}^{(3)}$ and $\Delta A_{Qg}^{(3)}$, 2403.00513 [hep-ph].
- J. Ablinger et al., The Single-Mass Variable Flavor Number Scheme at Three-Loop Order, DESY 24–037

The main time-line for the 3-loop corrections

- 2005 F_L [no massive 3-loop OMEs needed]
- 2010 All unpolarized N_F terms and $A_{qg,Q}^{(3)}, A_{qq,Q}^{(3),PS}$
- 2014 unpolarized logarithmic 3-loop contributions and $A_{gq,Q}^{(3)}, (\Delta)A_{qq,Q}^{(3),NS}, A_{Qq}^{(3),PS}$
- 2017 two-mass corrections $A_{gq,Q}^{(3)}, (\Delta)A_{qq,Q}^{(3),NS}, A_{Qq}^{(3),PS}$
- 2018 two-mass corrections $A_{gg,Q}^{(3)}$
- 2019 2-loop correction: $(\Delta)A_{Qq}^{(2),PS}$ whole kinematic region and $\Delta A_{Qq}^{(3),PS}$
- 2019 two-mass corrections $\Delta A_{Qq}^{(3),PS}$
- 2020 two-mass corrections $\Delta A_{gg,Q}^{(3)}$
- 2021 polarized logarithmic 3-loop contributions and $\Delta A_{qg,Q}^{(3)}, \Delta A_{qq,Q}^{(3),PS}, \Delta A_{gq}^{(3)}$
- 2022 3-loop polarized massless Wilson coefficients [JB, Marquard, Schneider, Schönwald]
- 2022 corrected the polarized 2-loop contributions
- 2022 $(\Delta)A_{gg,Q}^{(3)}$
- 2023 $(\Delta)A_{Qg}^{(3)}$: 1st order factorizing parts
- 2024 $(\Delta)A_{Qg}^{(3)}$, [two-mass corrections $(\Delta)A_{Qg}^{(3)}$]; **Project duration $\gtrsim 15$ years**

The Wilson Coefficients at large Q^2



$$L_{q,(2,L)}^{NS}(N_F + 1) = a_s^2 [A_{qq,Q}^{(2),NS}(N_F + 1)\delta_2 + \hat{C}_{q,(2,L)}^{(2),NS}(N_F)] + a_s^3 [A_{qq,Q}^{(3),NS}(N_F + 1)\delta_2 + A_{qq,Q}^{(2),NS}(N_F + 1)C_{q,(2,L)}^{(1),NS}(N_F + 1) + \hat{C}_{q,(2,L)}^{(3),NS}(N_F)]$$

$$L_{q,(2,L)}^{PS}(N_F + 1) = a_s^3 [A_{qq,Q}^{(3),PS}(N_F + 1)\delta_2 + N_F A_{qq,Q}^{(2),NS}(N_F) \tilde{C}_{g,(2,L)}^{(1),NS}(N_F + 1) + N_F \hat{C}_{q,(2,L)}^{(3),PS}(N_F)]$$

$$L_{g,(2,L)}^S(N_F + 1) = a_s^2 [A_{gg,Q}^{(1)}(N_F + 1)N_F \tilde{C}_{g,(2,L)}^{(2)}(N_F + 1) + a_s^3 [A_{gg,Q}^{(3)}(N_F + 1)\delta_2 + A_{gg,Q}^{(1)}(N_F + 1)N_F \tilde{C}_{g,(2,L)}^{(2)}(N_F + 1) + A_{gg,Q}^{(2)}(N_F + 1)N_F \tilde{C}_{g,(2,L)}^{(1)}(N_F + 1) + A_{Qg}^{(1)}(N_F + 1)N_F \tilde{C}_{q,(2,L)}^{(2),PS}(N_F + 1) + N_F \hat{C}_{g,(2,L)}^{(3)}(N_F)]$$

$$H_{q,(2,L)}^{PS}(N_F + 1) = a_s^2 [A_{Qq}^{(2),PS}(N_F + 1)\delta_2 + \tilde{C}_{q,(2,L)}^{(2),PS}(N_F + 1)] + a_s^3 [A_{Qq}^{(3),PS}(N_F + 1)\delta_2 + A_{qq,Q}^{(2)}(N_F + 1)\tilde{C}_{g,(1,L)}^{(2)}(N_F + 1) + A_{Qq}^{(2),PS}(N_F + 1)\tilde{C}_{q,(2,L)}^{(1),NS}(N_F + 1) + \tilde{C}_{q,(2,L)}^{(3),PS}(N_F + 1)]$$

$$H_{g,(2,L)}^S(N_F + 1) = a_s [A_{Qg}^{(1)}(N_F + 1)\delta_2 + \tilde{C}_{g,(2,L)}^{(1)}(N_F + 1)] + a_s^2 [A_{Qg}^{(2)}(N_F + 1)\delta_2 + A_{Qg}^{(1)}(N_F + 1)\tilde{C}_{q,(2,L)}^{(1)}(N_F + 1) + A_{gg,Q}^{(1)}(N_F + 1)\tilde{C}_{g,(2,L)}^{(1)}(N_F + 1) + \tilde{C}_{g,(2,L)}^{(2)}(N_F + 1)] + a_s^3 [A_{Qg}^{(3)}(N_F + 1)\delta_2 + A_{Qg}^{(2)}(N_F + 1)\tilde{C}_{q,(2,L)}^{(1)}(N_F + 1) + A_{gg,Q}^{(2)}(N_F + 1)\tilde{C}_{g,(2,L)}^{(1)}(N_F + 1) + A_{Qg}^{(1)}(N_F + 1)\tilde{C}_{q,(2,L)}^{(2),S}(N_F + 1) + A_{gg,Q}^{(1)}(N_F + 1)\tilde{C}_{g,(2,L)}^{(1)}(N_F + 1) + \tilde{C}_{g,(2,L)}^{(3)}(N_F + 1)]$$

- The case for two different masses obeys an analogous representation.
- Note the contributions of the **massless Wilson coefficients**.

The variable flavor number scheme



- Matching conditions for parton distribution functions:

$$f_k(N_F + 2) + \bar{f}_k(N_F + 2) = A_{qq,Q}^{\text{NS}} \left(N_F + 2, \frac{m_1^2}{\mu^2}, \frac{m_2^2}{\mu^2} \right) \cdot [f_k(N_F) + \bar{f}_k(N_F)] + \frac{1}{N_F} A_{qq,Q}^{\text{PS}} \left(N_F + 2, \frac{m_1^2}{\mu^2}, \frac{m_2^2}{\mu^2} \right) \cdot \Sigma(N_F) \\ + \frac{1}{N_F} A_{qg,Q} \left(N_F + 2, \frac{m_1^2}{\mu^2}, \frac{m_2^2}{\mu^2} \right) \cdot G(N_F),$$

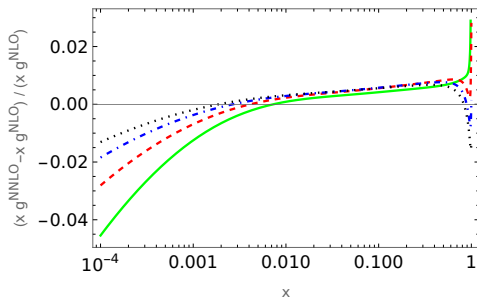
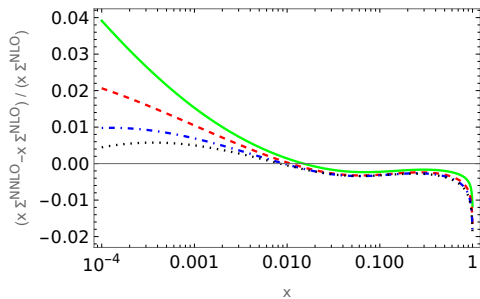
$$f_Q(N_F + 2) + \bar{f}_Q(N_F + 2) = A_{Qq}^{\text{PS}} \left(N_F + 2, \frac{m_1^2}{\mu^2}, \frac{m_2^2}{\mu^2} \right) \cdot \Sigma(N_F) + A_{Qg} \left(N_F + 2, \frac{m_1^2}{\mu^2}, \frac{m_2^2}{\mu^2} \right) \cdot G(N_F),$$

$$\Sigma(N_F + 2) = \left[A_{qq,Q}^{\text{NS}} \left(N_F + 2, \frac{m_1^2}{\mu^2}, \frac{m_2^2}{\mu^2} \right) + A_{qq,Q}^{\text{PS}} \left(N_F + 2, \frac{m_1^2}{\mu^2}, \frac{m_2^2}{\mu^2} \right) + A_{Qq}^{\text{PS}} \left(N_F + 2, \frac{m_1^2}{\mu^2}, \frac{m_2^2}{\mu^2} \right) \right] \cdot \Sigma(N_F) \\ + \left[A_{qg,Q} \left(N_F + 2, \frac{m_1^2}{\mu^2}, \frac{m_2^2}{\mu^2} \right) + A_{Qg} \left(N_F + 2, \frac{m_1^2}{\mu^2}, \frac{m_2^2}{\mu^2} \right) \right] \cdot G(N_F),$$

$$G(N_F + 2) = A_{gq,Q} \left(N_F + 2, \frac{m_1^2}{\mu^2}, \frac{m_2^2}{\mu^2} \right) \cdot \Sigma(N_F) + A_{gg,Q} \left(N_F + 2, \frac{m_1^2}{\mu^2}, \frac{m_2^2}{\mu^2} \right) \cdot G(N_F).$$

The charm and bottom quark masses are not that much different.

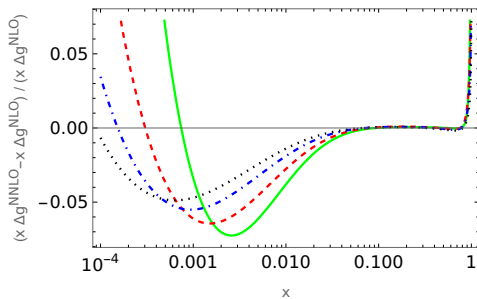
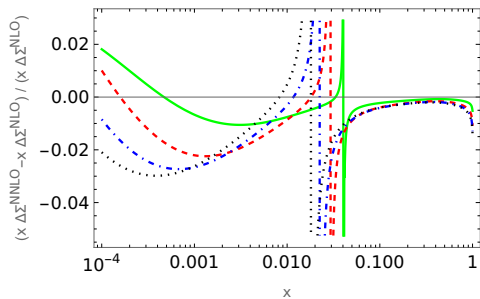
Relative effect in unpolarized NNLO evolution



$Q^2 = 10, 10^2, 10^3, 10^4 \text{ GeV}^2$ dotted, dash-dotted, dashed, full lines. [M. Saragnese, 2022]

The unpolarized world deep-inelastic data have a precision of $O(1\%)$.

Relative effect in polarized NNLO evolution



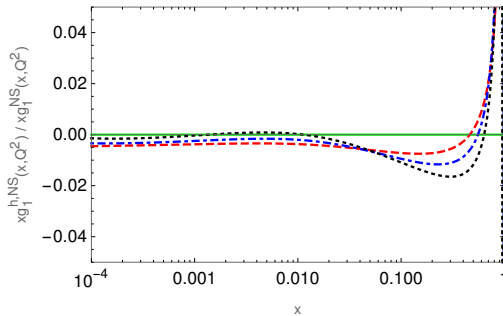
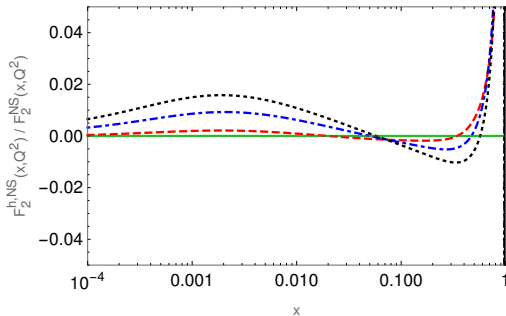
$Q^2 = 10, 10^2, 10^3, 10^4 \text{ GeV}^2$ dotted, dash-dotted, dashed, full lines. [M. Saragnese, 2022]

The future polarized data at the **EIC** will reach a precision of $O(1\%)$.

The relative contribution of HQ to non-singlet structure functions at N³LO

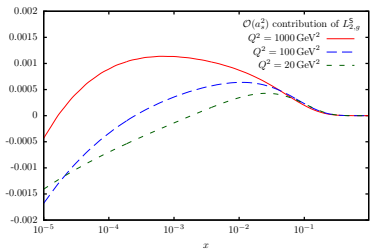


Scheme-invariant evolution

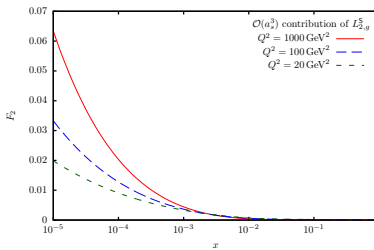


Left: The relative contribution of the heavy flavor contributions due to c and b quarks to the structure function F_2^{NS} at N³LO; dashed lines: 100 GeV²; dashed-dotted lines: 1000 GeV²; dotted lines: 10000 GeV². Right: The same for the structure function xg_1^{NS} at N³LO. [JB, M. Saragnese, 2021].

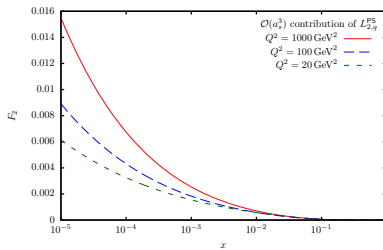
Numerical Results : $L_{g,2}^S$ and $L_{q,2}^{PS}$



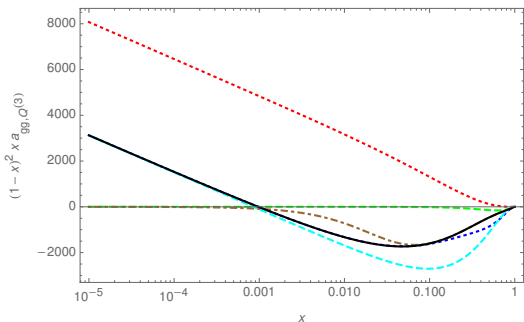
$\mathcal{O}(a_s^2) L_{2,g}^S$



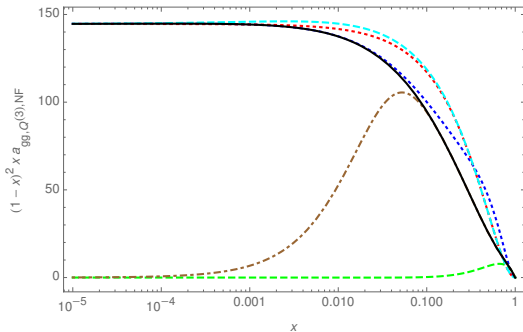
$\mathcal{O}(a_s^3) L_{2,g}^S$



$L_{q,2}^{PS}$

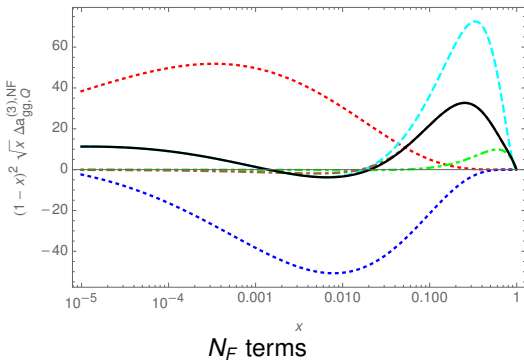
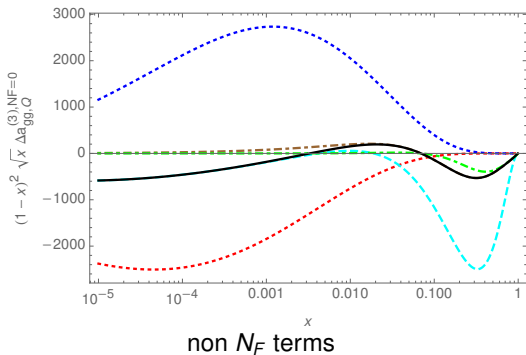


non N_F terms



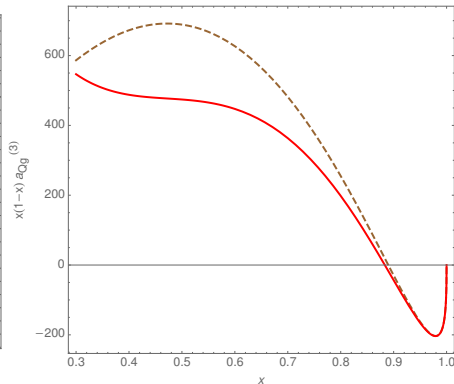
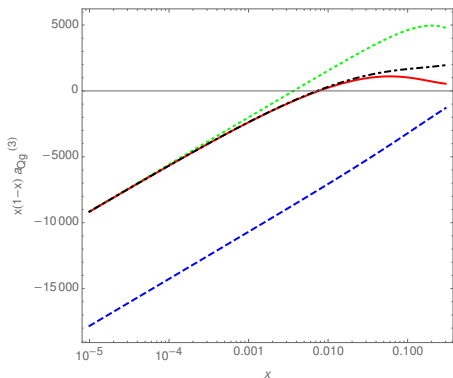
N_F terms

Left panel: The non- N_F terms of $a_{gg,Q}^{(3)}(N)$ (rescaled) as a function of x . Full line (black): complete result; upper dotted line (red): term $\propto \ln(x)/x$; lower dashed line (cyan): small x terms $\propto 1/x$; lower dotted line (blue): small x terms including all $\ln(x)$ terms up to the constant term; upper dashed line (green): large x contribution up to the constant term; dash-dotted line (brown): complete large x contribution. Right panel: the same for the N_F contribution.

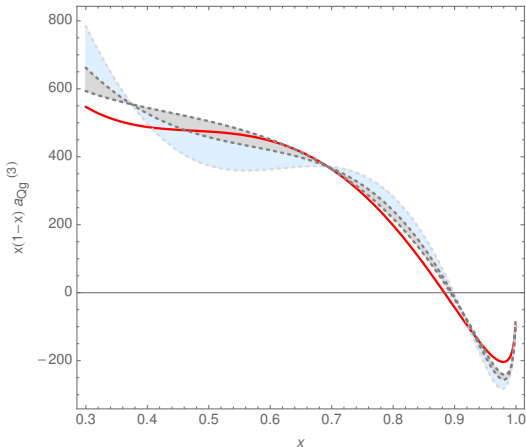
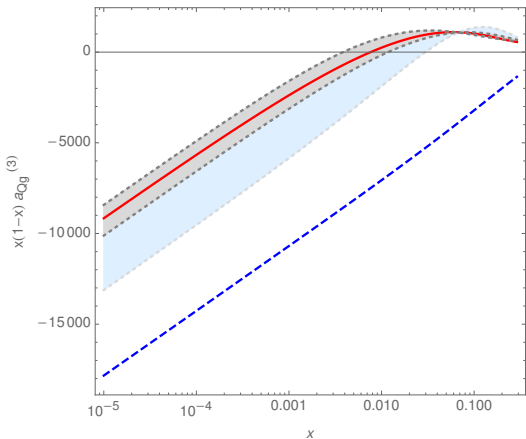


The non- N_F terms of $\Delta a_{gg,Q}^{(3)}(N)$ (rescaled) as a function of x . Full line (black): complete result; lower dotted line (red): term $\ln^5(x)$; upper dotted line (blue): small x terms $\propto \ln^5(x)$ and $\ln^4(x)$; upper dashed line (cyan): small x terms including all $\ln(x)$ terms up to the constant term; lower dash-dotted line (green): large x contribution up to the constant term; dash-dotted line (brown): full large x contribution. Right panel: the same for the N_F contribution.

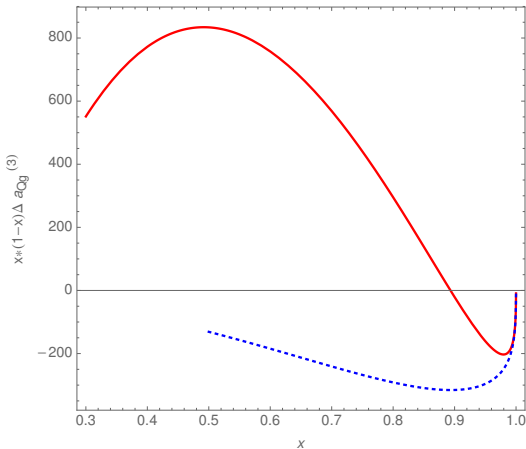
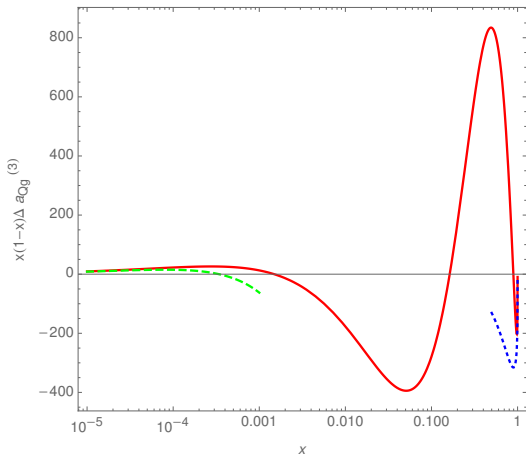
1009 of the total 1233 Feynman diagrams have first-order factorizing contributions only and are given by G -functions up to root-values letters. The letters for all constants can be rationalized.



$a_{Qg}^{(3)}(x)$ as a function of x , rescaled by the factor $x(1-x)$. Left panel: smaller x region. Full line (red): $a_{Qg}^{(3)}(x)$; dashed line (blue): leading small- x term $\propto \ln(x)/x$ [Catani, Ciafaloni, Hautmann, 1990]; dotted line (green): $\ln(x)/x$ and $1/x$ term; dash-dotted line (black): all small- x terms, including also $\ln^k(x)$, $k \in \{1, \dots, 5\}$. Right panel: larger x region. Full line (red): $a_{Qg}^{(3)}(x)$; dashed line (brown): leading large- x terms up to the terms $\propto (1-x)$, covering the logarithmic contributions of $O(\ln^k(1-x))$, $k \in \{1, 4\}$.

$a_{Qg}^{(3)}$ 

$a_{Qg}^{(3)}(x)$ as a function of x , rescaled by the factor $x(1-x)$. Left panel: smaller x region. Full line (red): $a_{Qg}^{(3)}(x)$; dashed line (blue): leading small- x term $\propto \ln(x)/x$ [Catani, Ciafaloni, Hautmann, 1990]; light blue region: estimates of [Kawamura et al., 2012]; gray region: estimates of [ABMP 2017]. Right panel: larger x region. Full line (red): $a_{Qg}^{(3)}(x)$; light blue region: estimates of [Kawamura et al., 2012] gray region: estimates of [ABMP 2017].

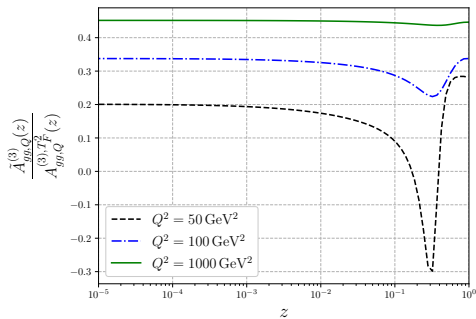


$\Delta a_{Qg}^{(3)}(x)$ as a function of x , rescaled by the factor $x(1-x)$. Left panel: full line (red): $\Delta a_{Qg}^{(3)}(x)$; dashed line (green): the small- x terms $\ln^k(x)$, $k \in \{1, \dots, 5\}$; dotted line (blue): the large- x terms $\ln^l(1-x)$, $l \in \{1, \dots, 4\}$. Right panel: larger x region. Full line (red): $\Delta a_{Qg}^{(3)}(x)$; dotted line (blue): the large- x terms $\ln^l(1-x)$, $l \in \{1, \dots, 4\}$.

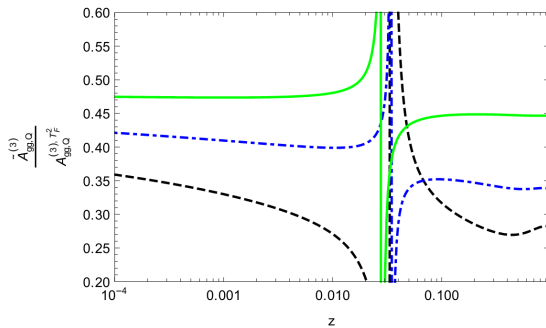
Two-mass Results: $\tilde{A}_{gg,Q}^{(3)}$



The two mass contributions over the whole T_F^2 -contributions to the OME $\tilde{A}_{gg,Q}^{(3)}$:

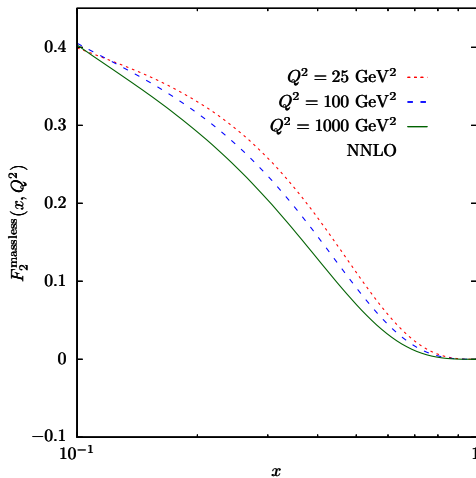
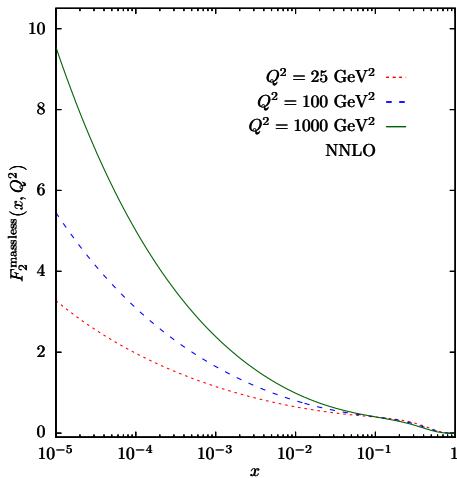


unpolarized



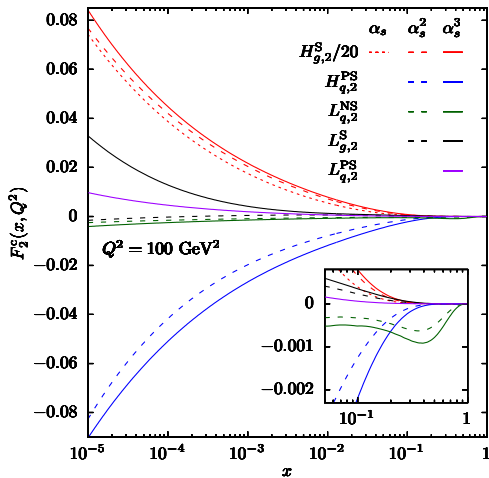
polarized

The massless contributions to F_2



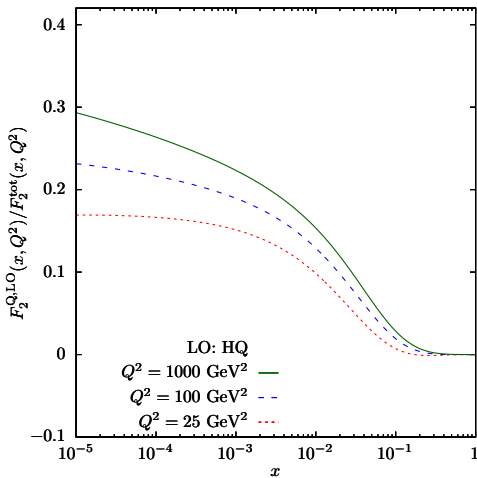
$N_F = 3$ massless quarks.

Single-mass contributions to $F_2^{c,b}$



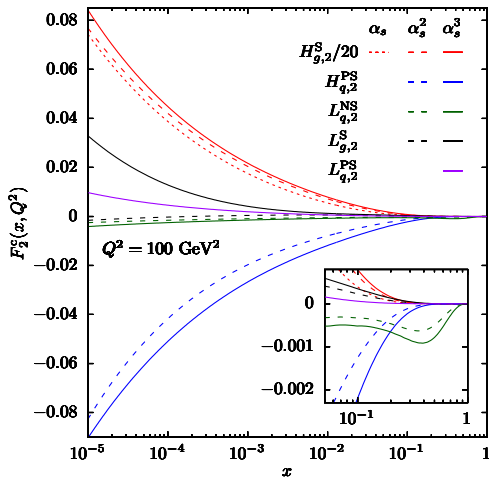
charm for $Q^2 = 100 \text{ GeV}^2$.

Allows to strongly reduce the current theory error on m_c .

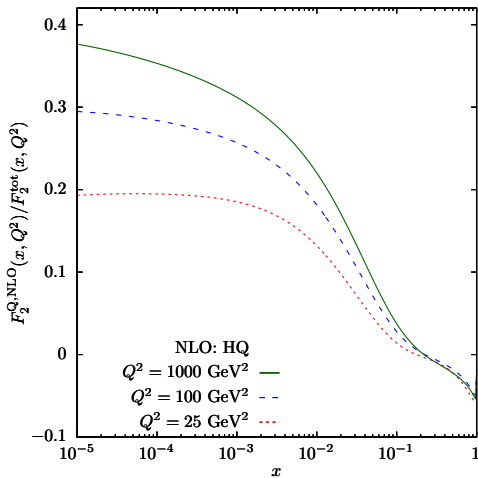


c and b single mass contributions

Single-mass contributions to $F_2^{c,b}$



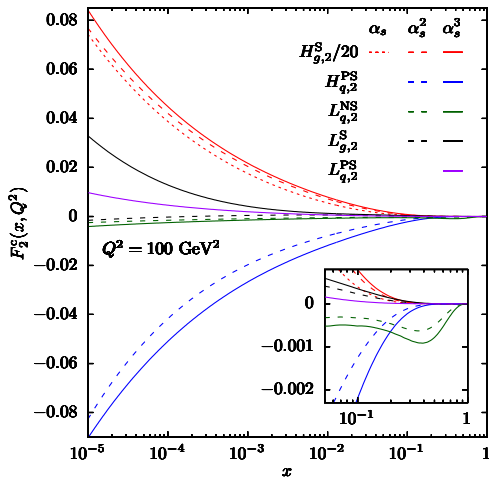
charm for $Q^2 = 100 \text{ GeV}^2$.



c and b single mass contributions

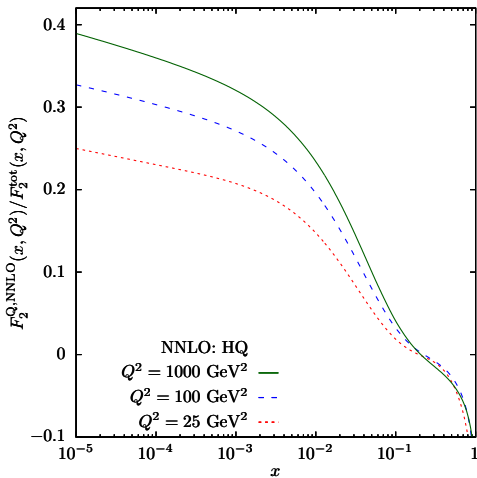
Allows to strongly reduce the current theory error on m_c .

Single-mass contributions to $F_2^{c,b}$



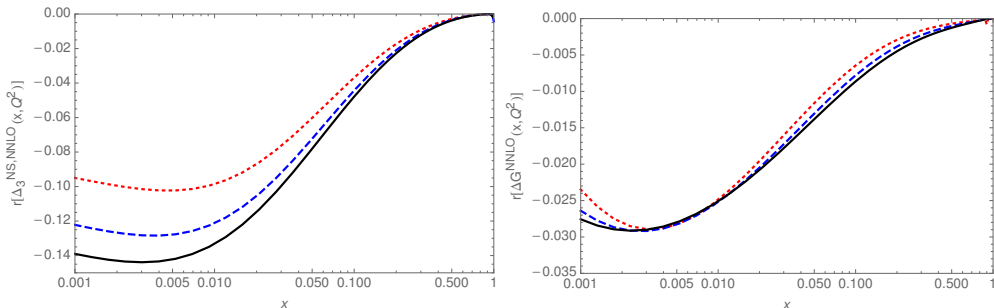
charm for $Q^2 = 100 \text{ GeV}^2$.

Allows to strongly reduce the current theory error on m_c .



c and b single mass contributions

Polarized PDF evolution in the Larin Scheme



[Dotted line: $Q^2 = 100 \text{ GeV}^2$, dashed line: $Q^2 = 1000 \text{ GeV}^2$, full line: $Q^2 = 10000 \text{ GeV}^2$]

$$r(x, Q^2) = \frac{f^L(x, Q^2)}{f^M(x, Q^2)} - 1$$

The pdfs are necessary to match HO Larin-scheme calculations.

Conclusions



- All unpolarized and polarized **single-mass** OMEs and the associated massive Wilson coefficients for $Q^2 \gg m_Q^2$ have been calculated. The unpolarized and **polarized** massless three-loop Wilson coefficients were calculated and contribute to the present results.
- The calculation of all unpolarized and polarized **two-mass OMEs**, except for $(\Delta)A_{Qg}^{(3)}$, are finished and the remaining OMEs will be available very soon.
- Various new **mathematical and technological** methods were developed during the present project. They are available for use in further single- and two-mass calculations in other QFT projects.
- Very soon new precision analyses of the world DIS-data to measure $\alpha_s(M_Z)$ and m_c at higher precision can be carried out.
- Both the single- and two-mass **VFNS at 3-loop** order will be available in form of a numerical program, to be used e.g. in applications at hadron colliders.
- The results in the **polarized case** prepare the analysis of the precision data, which will be taken at the **EIC** starting at the end of this decade.
- For all sub-processes it turned out that the small x **BFKL approaches fail** to present the physical result due to quite a series of missing subleading terms, which substantially correct the LO behaviour. The correct description requires the full calculation.